Publication II

Immobilization−Stabilization of Proteins on Nanofibrillated Cellulose Derivatives and Their Bioactive Film Formation. Suvi Arola, Tekla Tammelin, Harri Setälä, Antti Tullila and Markus B. Linder. *Biomacromolecues,* 2012, 13 (3), pp. 594–603. DOI: 10.1021/bm201676q

Article

pubs.acs.org/Biomac

Immobilization–Stabilization of Proteins on Nanofibrillated Cellulose Derivatives and Their Bioactive Film Formation

Suvi Arola,*[,†,‡] Tekla Tammelin,[§] Harri Setälä,[§] Antti Tullila,[†] and Markus B. Linder[†]

[†]VTT, Technical Research Centre of Finland, Bio and Process Technology, Tietotie 2, P.O. Box 1000, FIN-02044 VTT, Finland

[§]VTT, Technical Research Centre of Finland, Energy and Pulp and Paper, Biologinkuja 7, P.O. Box 1000, FIN-02044 VTT, Finland

[‡]Department of Applied Physics, Aalto University School of Science and Technology, P.O. Box 15100, FI-00076 Aalto, Finland

Supporting Information

ABSTRACT: In a number of different applications for enzymes and specific binding proteins a key technology is the immobilization of these proteins to different types of supports. In this work we describe a concept for protein immobilization that is based on nanofibrillated cellulose (NFC). NFC is a form of cellulose where fibers have been disintegrated into fibrils that are only a few nanometers in diameter and have a very large aspect ratio. Proteins were conjugated through three different strategies using amine, epoxy, and carboxylic acid functionalized NFC. The conjugation chemistries were chosen according to the reactive groups on the NFC derivatives; epoxy amination, heterobifunctional modification of amino groups, and EDC/s-NHS activation of carboxylic acid groups. The conjugation reactions were performed in solution and immobilization was performed by spin coating the protein–NCF conjugates. The structure of NFC was shown to be advantageous for both protein performance and stability. The use of NFC allows all covalent chemistry to be performed in solution, while the immobilization is achieved by a simple spin coating or spreading of the protein–NFC conjugates on a support. This allows more scalable methods and better control of conditions compared to the traditional methods that depend on surface reactions.

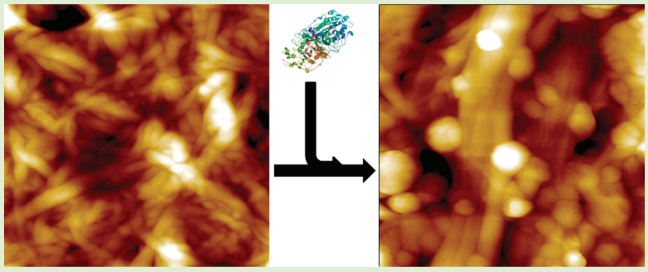

INTRODUCTION

The immobilization of proteins and other biomolecules is an essential technique in several biotechnical applications.[1−4] For the use of enzymes to catalyze industrial processes, immobilization enables enzyme reuse, continuous processes, and can markedly increase their stability. Diagnostic applications also rely largely on immobilization of antigens or antibodies using a number of different formats from microtiter plates to different types of strips. There is a continuous need to improve and diversify technologies for immobilization for the development of new formats, better economy, and performance.[2,4] Several techniques have been developed for protein immobilization. These can broadly be grouped in the following categories based on mechanisms: (i) physical interactions or adsorption, (ii) chemical covalent bonds, or (iii) high affinity interactions between biological molecules.[4] For industrial enzymes the most preferred method for immobilization is the use of covalent coupling. For this, great efforts have been made to produce feasible protocols that yield reproducible results and stabile enzymes.[3,5] It has been found that the environment around and on the solid support as well as the chemistry used in the immobilization have a great impact on the stability and performance of the enzymes.[2] In most cases, the molecules to be immobilized are covalently coupled directly onto the solid supports. With this approach it is often found that the efficiency of immobilization is restricted by the surface chemistry of the immobilization platform.[5,6] Also, the fact that the immobilization often occurs randomly in respect to protein orientation is one of the drawbacks of these systems. Proteins tend to unfold when they are assembled on surfaces, which leads to loss of activity.[4] Another drawback is that procedures for direct covalent linking on surfaces can be problematic to scale for large areas.

Cellulose has been studied as a carrier material for protein immobilization previously mostly because of the possibility to use specific cellulose-binding proteins that bind and therefore immobilize spontaneously to cellulose materials.[7] In other cases, different types of regenerated celluloses have been used as a carriers.[8] In this work, we take advantage of recent developments in cellulose technology to design new techniques for surface immobilization of biomolecules. Cellulose is a homopolymer formed by repeating units of D-glucose linked together by β-(1−4) glycosidic bonds. In natural cellulose materials, such as wood, the polymer chains are packed together to form elemental fibrils with a cross-section of 3−5 nm. These elemental fibrils are usually considered to be the lowest level of hierarchy in cellulose assembly.[9] In the wood structure, these elemental fibrils are packed further to form

Received: July 4, 2011
Revised: January 13, 2012
Published: January 17, 2012

microfibrils that range in size from 15−20 nm which further aggregate in to larger fibril bundles and finally to wood fibers.[10,11] It has been shown that cellulose pulp can be disintegrated to the nanosized microfibrils with mechanical and biological methods and in this context the term nanofibrillated cellulose (NFC) has also been adopted.[12,13] The very long aspect ratio and the high stiffness of the fibrils are important for giving NFC its properties. The surface of the fibrils are dominated by hydroxyl groups that make the surface hydrophilic, but also result in hydrogen bonding interactions between adjacent fibrils. These properties lead to gel formation in aqueous suspensions that are strongly stabilized by these network interactions. Already, at 2% dry weight, such suspensions have a very high viscosity, leading to applications of NFC as rheology modifiers and in the dried form as aerogels.[14−17] The gel-like behavior also makes NFC difficult to handle at high concentrations. Other applications that take advantage of the properties of NFC are in nanocomposite materials as reinforcing elements and as templates for functional nanostructures.[14,18−20] NFC also has an ability to form strong thin films that have nanoporous structures and good adhesion to underlying structures.[14,21−23] The film forming capabilities also depend on strong fibril networks that are formed by the characteristic properties of high aspect ratio, stiffness of the fibrils and interacting hydroxyl groups.[21] NFC thin films are readily made, for example, by spin coating from aqueous media and have been used as model films to study native cellulose I behavior at surfaces.[21,24] It has also been shown that NFC films can be used as paper coatings to reinforce paper and increase the barrier properties such as air permeability.[25,26]

Due to the high amount of reactive hydroxyl groups on the fibril surface, NFC has an ability to absorb more water than other cellulose model films.[21] The hydroxyl groups on the surface of the fibrils also provide possibilities for chemical modifications of the NFC. One very efficient way of modifying surface hydroxyl groups is through oxidation using TEMPO (2,2,6,6-tetramethylpiperidine-1-oxyl), resulting in the formation of carboxyl groups on the fibril surface.[27,28] The reaction also leads to a more easy disintegration, giving very thin fibrils with a diameter of 3−5 nm[27,28] but which also have altered properties due to their high negative charge on the surface.

The possibility to covalently modify and the efficient film forming properties of NFC inspired us to investigate how NFC would function as a support for protein immobilization. The advantage of this approach is that the conjugation reactions could be performed in solution compared to the conventional methods that use surface chemistry, making the reactions more reproducible and scalable. After the conjugation reaction, the protein immobilization to the solid support could be achieved by different spreading techniques such as spin coating. The ability of cellulose to take up water is also pronounced in NFC, which is likely to be advantageous for immobilized proteins.[3]

In this work, we investigated the effect of different conjugation strategies and, for that, three different NFC derivatives were made: epoxy functionalized, amine functionalized, and carboxylic acid functionalized NFC. The three different NFC derivatives demanded different conjugation strategies. As model proteins, we used alkaline phosphatase (AP) and anti-hydrocortisone antibody. The two proteins used in this study were chosen for their specific bioactivities but also because of the difference in their substrate size. AP gives a colored reaction with a soluble substrate that has a small size compared to proteins. Anti-hydrocortisone antibody on the other hand is more relevant in its bioactivity to recognize hydrocortisone.

EXPERIMENTAL SECTION

Materials and Methods. *Preparation of Epoxy Functionalized Nanofibrillated Cellulose (epoxy-NFC).* The first step for the epoxy functionalization of cellulose was through an allylation step. Briefly, 250 mL of butyl glycidyl ether and 100 mL of allyl glycidyl ether were added to 500 g of never-dried bleached birch kraft pulp fibers (29.1%) in 90% aqueous *t*-butanol (1.5 L) in alkaline conditions (114 mL, 10 M NaOH + 600 mL water) at 60 °C overnight. Sulfuric acid was then added until the pH was 7. The fibers were washed with ethanol and water by filtration and then ground using a Masuko refiner (Masuko Sangyo, Japan). The obtained microfibrillated cellulose (MFC, dry matter content 2−3%) was then repeatedly centrifuged and washed by resuspending with acetone. After this solvent exchange step, the dry matter content was 6.0% and water content 2−5%. Next, allyl glycidyl ether (3 mol/L mol anhydroglucose unit (AGU)) was added to 165 g of the solvent-exchanged MFC and allowed to react at 65 °C overnight. Fibers were filtered and washed with ethanol and water. The degree of substitution was determined by ^{13}C cross-polarized magic angle spinning nuclear magnetic resonance (CP/MAS NMR) spectroscopy[29] and also by a method published by Heinze et al.,[30] where allyl groups were brominated and the bromine content was determined.

The epoxy functionalization of allylated MFC was performed using the procedure published by Huijbrechts and et al.[31] Allylated MFC (dry matter content 4.7%) was reacted in sodium carbonate/bicarbonate buffer solution with acetonitrile and 30% hydrogen peroxide overnight at 30 °C. The cellulose was separated by filtration, and washed with water and ethanol to yield epoxy-MFC. The epoxy content of epoxy-MFC was analyzed using the slightly modified method published by Huijbrechts et al.[31] Freeze-dried epoxy-MFC fibers were suspended in water and reacted with 4,4′-diaminodiphenylmethane in ethanol overnight at 30 °C. The product was isolated by centrifugation, and washed with ethanol and water. The DS value for epoxy groups was calculated from the amount of nitrogen analyzed by the Kjeldahl method (Vario MAX CHN, Maxitech Corporation, Pakistan). Epoxy-MFC was then fluidized to nanofibrillated cellulose (NFC) with a pressure of 1600 bar and 15 passes (M110EH, Microfluidics, MA, U.S.A.) to yield epoxy-NFC (dry matter content 1.6%).

Preparation of Amine-Functionalized Nanofibrillated Cellulose (amine-NFC). Never-dried bleached birch kraft pulp was fluidized (dry matter content ∼2%) with a pressure of 1600 bar with eight passes as described above to give NFC. The solvent for NFC was exchanged via acetone to dimethyl acetamide (DMA) by five centrifugation and redispersing steps for each solvent. Amine functionalization was conducted via silylation reactions using a protocol originally tailored for dissolved cellulose.[32−34] First, 0.75 g of solvent-exchanged NFC was suspended into 100 mL of DMA. Nitrogen was bubbled into the suspension for 1 h after which it was heated to 80 °C. Then, 15 mL of 3-aminopropyl trimethoxysilane was added and the reaction was allowed to proceed overnight at 80 °C. The product was washed by centrifugation and redispersed with methanol. Finally, the solvent for amine-NFC was exchanged to water by centrifuging and redispersing five times. The degree of amine functionalization was calculated from the surface silicon and surface nitrogen content analyzed by x-ray photoelectron spectroscopy (XPS), as described in Johansson et al.[35,36] The dry matter content of the resulting amine-NFC was 1.6%.

Preparation of 2,2,6,6,-Tetramethylpiperidine-1-oxyl Oxidized Nanofibrillated Cellulose (TEMPO-NFC). NFC functionalized with carboxylic acid groups (TEMPO-NFC) was prepared as described by Saito et al.[28] Shortly, never-dried, bleached birch pulp at 1 g L^{-1} concentration was subjected to 2,2,6,6-tetramethylpiperidine-1-oxyl (TEMPO)-catalyzed oxidization (0.3 weight ratio of TEMPO to pulp) for 4 h at room temperature. The product was purified from residual reaction chemicals by centrifugation and redispersing with deionized

Scheme 1. Reaction Schemes of Alkaline Phosphatase Conjugation to Different NFC Derivatives[a]

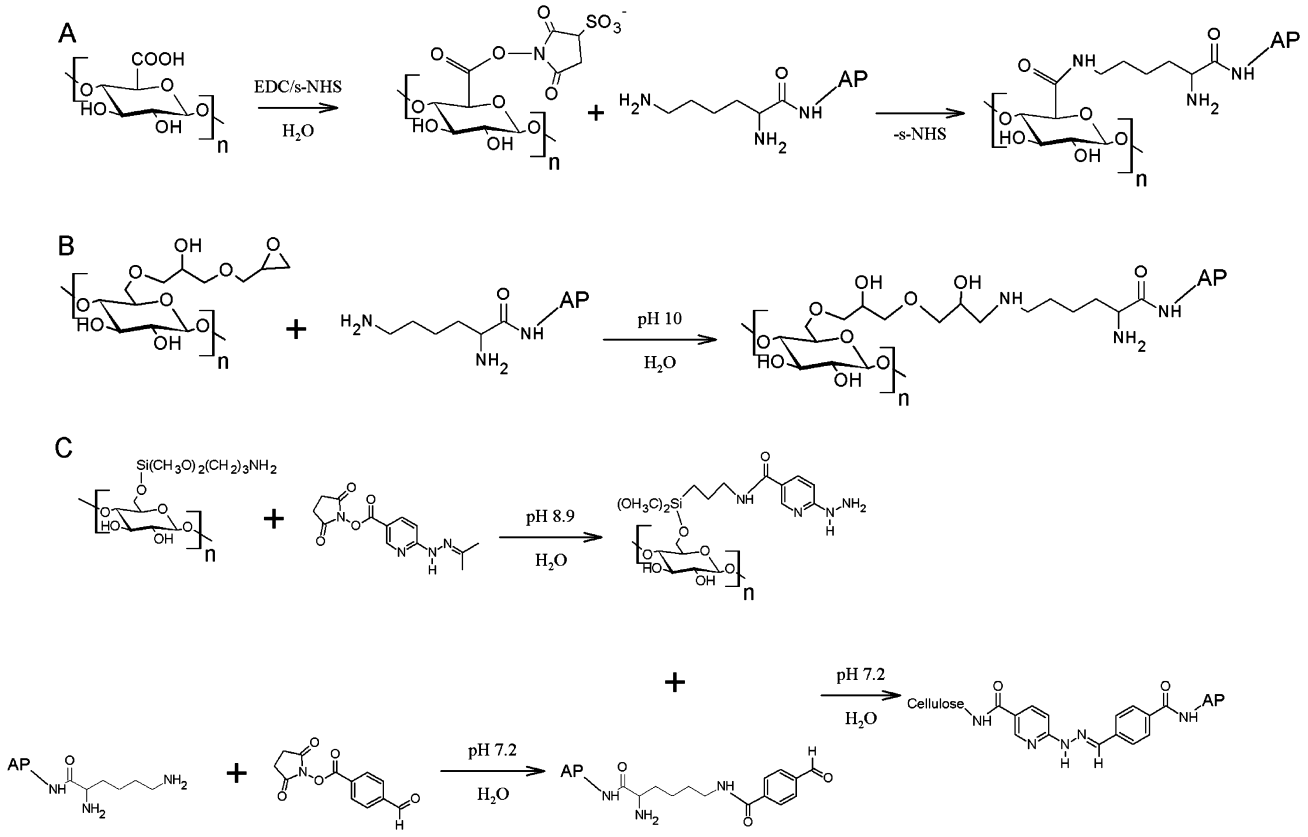

[a](A) Reaction of lysine residues on AP surface with epoxy groups on epoxy-NFC through a ring-opening reaction. (B) Carboxylic acid groups on TEMPO−NFC were first activated using EDC and s-NHS. The activated carboxylic acid groups react with lysine groups on AP forming stabile peptide bonds. (C) Amino groups on amine-NFC were modified with SANH to yield hydrazine/hydrazide reactive species (SANH−NFC). Lysine groups on AP were reacted with SFB to yield an aldehyde modified AP (SFB−AP). The aldehyde on SFB−AP and the hydrazine/hydrazide on SANH−NFC reacted forming a stabile hydrazone bond.

water. The centrifugation and washing step was repeated twice. The resulting TEMPO-NFC was then fluidized twice using 1300 and 1900 bar pressure, respectively, with a fluidizer (Microfluidics M110EH). The DS value for TEMPO-NFC (dry matter content 0.9%) was determined by conductometric titration of carboxylic acid groups.

Conjugation of AP to Epoxy−NFC. The reaction was performed through epoxy amination in alkaline conditions where the amino groups of lysine amino acids on the enzyme alkaline phosphatase (AP; Sigma, P5931-500U) react with the epoxy group of epoxy-NFC in a ring-opening reaction (Scheme 1A).[37] A total of 200 μg of AP (final concentration 7.9 μM) was reacted with 600 μg of epoxy-NFC (final concentration 1.13 g L^{-1}) in 0.1 M $NaHCO_3/Na_2CO_3$ pH 10 buffer for 24 h at 22 °C. Negative controls for the conjugation were made by first blocking the epoxy groups with excess of diethanolamine (DEA, final concentration of 1 M) and then reacting them with AP. The effect of 0.5 μL of catalyst triethylamine was tested for the epoxy amination reaction.

Conjugation of AP to TEMPO−NFC. AP was coupled to TEMPO-NFC through a peptide bond forming reaction (Scheme 1B).[37] A minor amount of aldehyde groups are present on TEMPO-NFC and may react through a different reaction mechanism than that of carboxylic acids.[38] A 1:2.5 molar ratio mixture of 1-ethyl-3-[3-dimethylaminopropyl]carbodiimide hydrochloride (EDC, Pierce 22980, final concentration 2.5 mM) and *N*-hydroxysulfosuccinimide (s-NHS, Pierce 24510, final concentration 5 mM) was reacted with 53.2 μg of TEMPO-NFC (final concentration 0.133 g L^{-1}) in aqueous solution, pH ∼ 5, for 15 min at 22 °C. Activated TEMPO-NFC (final concentration 0.1 g L^{-1}) and AP (final concentration of 7.9 μM) were then conjugated by mixing in 25 mM borate buffer pH 8 for 3 h at 22 °C. A negative control was made by leaving out EDC and s-NHS and performing reactions otherwise, as described above.

Conjugation of AP to Amine−NFC. The conjugation of AP to amine-NFC was performed by a three-step reaction procedure (Scheme 1C).[39] First, 2 mL of 1.5 g L^{-1} amine-NFC in 25 mM borate buffer pH 8.9 was reacted with 10 μL of 20 g L^{-1} succinimidyl-4-hydrazinonicotinate acetone hydrazone (SANH, Thermo Scientific 22400) dissolved in dimethylsulfoxide (DMSO) for 3 h at 22 °C to yield a hydrazine/hydrazide reactive species on the amine-NFC (later referred to as SANH-NFC). The SANH-NFC was washed with Milli-Q water using a concentration tube (Amicon Ultra 10K 4 mL, Millipore). The benzaldehyde reactive AP (later referred to as SFB−AP) was made by mixing 250 μL of 3.2 g L^{-1} AP in phosphate buffer saline (PBS) pH 7.2 and 5 μL of 20 g L^{-1} succinimidyl-4-formylbenzoate (SFB, Thermo Scientific 2249) in DMSO for 3 h at 22 °C. The SFB−AP was washed with Milli-Q water as above (Amicon Ultra 10K 0.5 mL, Millipore). In the final step of the conjugation reaction, SFB−AP (0.14 g L^{-1}) and SANH-NFC (1.13 g L^{-1}) were allowed to react in PBS pH 7.2 overnight at 22 °C. Residual amine reactive groups were quenched by adding 1 M Tris buffer saline (TBS) pH 7.2 to a final concentration of 0.1 M and incubating for 65 h at +4 °C. Control samples were made using unmodified AP and amine-NFC in the final step.

Matrix-assisted laser desorption/ionization−time-of-flight mass spectrometry (MALDI−TOF MS, Bruker autoflex II MALDI−TOF) was used to study the extent of SFB modification of AP as described in Supporting Information (S1).

Preparation of Bioactive Films from AP−NFC Conjugates. AP−NFC films were prepared by spin coating a 50 μL aliquot of the different conjugates onto a silicon surfaces (Okmetic Oy, Vantaa,

Finland, 1 cm^2 pieces). Prior to use, the silica surfaces were washed three times with ethanol and Milli-Q water, dried in nitrogen flow, and spin coated with 50 μL of 1 g L^{-1} polyethyleneimine (PEI, Sigma-Aldrich) in water using an Autolab spin coater (Autolab, The Netherlands). PEI was used as an anchoring polymer to ensure sufficient adherence of NFC to the silica surface.[21] The procedure of spin coating the AP−NFC conjugates was repeated 1−11 times. After immobilization of AP−NFC films, the surfaces were washed (3 × 2 mL) for 3−4 h with buffer (0.1 M TRIS 50 mM $MgSO_4$ 0.2 M NaCl buffer pH 8.8) to remove noncovalently bound AP.

Determining Enzymatic Activity of AP−NFC Bioactive Films. The enzymatic activity of AP−NFC films was measured using a small chromogenic substrate 4-nitrophenyl phosphate sodium hexahydrate (*p*-NPP). A total of 500 μL of enzyme reaction buffer (0.1 M TRIS 50 mM $MgSO_4$ pH 8.8) and 500 μL of freshly prepared solution of *p*-NPP (2 g L^{-1}) in diethanolamine $MgCl_2$ buffer (Reagena Oy Ltd., Finland) was incubated with NFC film samples that had been spin coated on silicon surfaces. Absorbance at 405 nm of the enzyme reaction solution at a specific time points were measured with a spectrophotometer (Varioscan, Thermo Electron Corporation), and the amount of AP was calculated using a standard curve determined for nonconjugated AP in solution.

Long-Term Stability of AP on Different AP−NFC Films. To study if the conjugation of AP to the different NFC derivatives affected the stability of AP, the enzymatic activity of a series of samples incubated at elevated temperatures were studied. Silicon surfaces having two spin coated layers of all three different AP−NFC conjugates were kept in enzyme reaction buffer at either room temperature or +37 °C. The enzymatic activity of the films was measured at time points of 16, 24, 48, and 168 h. Solutions of AP (0.43 μM) in enzyme reaction buffer were used as controls and they were stored in the same conditions and enzyme reaction were performed similarly as to immobilized AP.

Conjugation of Hydrocortisone to AP. Hydrocortisone 3-oxime (Sigma-Aldrich, H6635) was conjugated to AP using EDC and s-NHS (Thermo Scientific, 22980 and 24510, respectively) as above. The formed hydrocortisone−AP conjugate was purified from unreacted hydrocortisone 3-oxime, EDC, and s-NHS using desalting column. Protein concentrations were measured using BCA Protein Assay Kit (Pierce, 23225). MALDI-TOF MS was applied to determine the extent of chemical conjugation degree of the haptens to the carrier protein as described previously for SFB−AP (Supporting Information, S1).

Production and Purification of Anti-Hydrocortisone Antibody. An anti-hydrocortisone Fab-fragment antibody (anti-hydrocortisone antibody) that had been selected from immunized mouse antibody phage display library against the hydrocortisone−AP conjugate was used.[40,41] The hydrocortisone specific antibody fragment clone, anti-hydrocortisone, was cloned into pKKtac expression vector containing His_6 tag for Fab-protein purification.[42] Protein production of anti-hydrocortisone Fab fragment was performed in *Escherichia coli* bacteria strain RV308 (ATCC 31608) and purified by metal affinity chromatography[43] followed by dialysis into PBS.

Conjugation of Anti-Hydrocortisone Antibody to TEMPO-NFC and Its Immobilization onto Solid Support. The antibody conjugation and immobilization was performed as described for AP above. Briefly, 200 μL of 0.133 g L^{-1} EDC/s-NHS activated TEMPO−NFC and 100 μg of anti-hydrocortisone antibody were reacted in PBS buffer pH 7.2 for 4 h at 22 °C. Bioactive films were spin coated as described above for AP−NFC conjugates. Silicon surfaces having one or two layers of antibody−NFC conjugate were prepared. One or two layers of only TEMPO−NFC were also spin coated as negative controls. The conjugation of antibody to TEMPO−NFC was studied by how much antigen was bound to the surfaces. The antigen, that is, hydrocortisone, had been conjugated to AP to facilitate its detection. The antibody-NFC surfaces were incubated with 100 μL of hydrocortisone−AP conjugate (10 mg L^{-1}) in PBS buffer pH 7.2 for 2 h at 22 °C and washed with of PBS buffer pH 7.2 overnight at +4 °C to remove any nonspecifically bound hydrocortisone−AP conjugate. The activity of AP bound to antibody-NFC surfaces was detected as previously described for immobilized AP.

Atomic Force Microscopy (AFM) Imaging. AFM was used to analyze the morphology of the NFC derivatives before and after AP conjugation and immobilization. AFM was also used to characterize the structural features of the different NFC derivatives. A NanoScope IIIa Multimode AFM instrument (E-scanner and J-scanner, Digital Instruments/Veeco) was used with an NSCI5/AlBS cantilever (μMASCH, U.S.A.). All images were recorded in tapping mode in air with scan rates of 0.8−1 Hz (free amplitude was about 0.65 V). The damping ratio was around 0.7−0.85. Images were flattened to remove possible tilts in the image data. Otherwise, no further processing of the images was done.

Quartz Crystal Microbalance with Dissipation (QCM-D). QCM-D (E4 instrument, Q-Sense AB, Sweden) was used to determine nonspecific adsorption of proteins to unmodified NFC surfaces and PEI surfaces. With QCM-D, the changes in frequency (Δf) and dissipation (ΔD), that is, changes in mass and viscoelastic properties on the sensor surface, are followed simultaneously as a function of time at the fundamental resonance frequency (5 MHz) and its overtones. The interpretation of QCM-D data has been discussed in detail elsewhere.[44,45] Quartz crystals coated with silica (QSX 303, mass sensitivity constant C = 0.177 mg m^{-2} Hz^{-1}) were used. Prior to use, the sensor crystals were washed for 30 min at room temperature in 2% SDS solution, rinsed with Milli-Q water, and dried in a nitrogen flow. The NFC layers were spin coated with NFC prepared as described previously.[19] The proteins studied were AP, bovine serum albumin (BSA), SFB−AP and hydrocortisone−AP conjugates. Spin-coated crystals were stabilized in the QCM-D chambers for 24 h against PBS buffer pH 7.2 before the measurements were started. The nonspecific protein binding of all the four proteins were tested on both PEI and NFC.

RESULTS

Estimation of the Degree of Substitution for Epoxy-Functionalized NFC. The functionalization of NFC was characterized by ^{13}C CP/MAS NMR and the Kjeldahl method. The first allylation step lead to the removal of approximately 40% of hemicelluloses and a 0.01 degree of substitution (DS) for modification by butyl and allyl functionalities, as determined by ^{13}C CP/MAS NMR (see Supporting Information, Figure S2). The final degree of substitution after second allylation step was estimated by integrating the combined area of both peaks from allyl groups and the area of the anomeric C1 carbon in cellulose (see Supporting Information, Figure S2). Because the NMR results are semiquantitative, they were verified for the final product using bromination of double bonds, as described by Heinze et al.[30] The results of both methods agreed well and gave the DS values for allyl groups after two allylation steps of 0.055 by NMR and 0.066 by bromination. The subsequent functionalization of allyl groups to epoxy groups was followed by the Kjeldahl method. For this measurement epoxy groups were first aminated. According to this method the amount of epoxy groups was 0.64 mmol g^{-1} cellulose and corresponds to a degree of substitution for epoxy groups 0.061 (Table 1). The results show that the allyl groups were converted to epoxy groups almost quantitatively.

Estimation of the Degree of Substitution for Amine-Functionalized NFC. XPS was used for the determination of the DS[35,36] for silylated amine modified NFC. XPS spectra and data are shown in Supporting Information, Figure S3 and Table S3. The degree of amination on the fibril surface was calculated from the nitrogen and silicon content. The surface content of nitrogen was 1.7% and the surface content of silicon was 1.5%, corresponding to surface substitution values of 0.21 for the nitrogen marker and 0.19 for the silica marker (Table 1). The degree of substitution was calculated to be 1.24 mmol of functional groups per gram of cellulose.

Table 1. Different Functionalizations of NFC, the DS Values Obtained for the Different Derivatives and the Degree of Derivatization in Relation to the Total Amount of Cellulose

Functionalized NFC	Degree of substitution (maximum DS)	Degree of derivatization (mmol g^{-1} cellulose)
Epoxy functionalized NFC 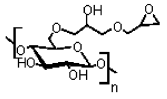	DS_{epoxy} 0.061 (DS_{max} = 3)[a] DS_{allyl} 0.066 (DS_{max} = 3)[b] DS_{allyl} 0.055 (DS_{max} = 3)[c]	0.64[g]
Amine functionalized NFC 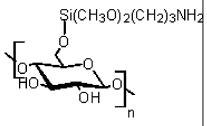	DS_{Si} ~0.2 (DS_{max} = 3)[d] DS_N ~0.2 (DS_{max} = 3)[e]	1.24[h]
TEMPO oxidized NFC 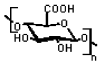	Surface charge ~0.9 meq g^{-1} pulp, corresponds to 57% efficiency in oxidation of C–6 hydroxyls of wood cellulose crystal[f]	0.9[i]

[a]Degree of substitution for epoxy groups per anhydroglucose units (AGUs) calculated from results of Kjeldahl method. [b]DS for allyl groups per AGU determined by ^{13}C/CP MAS NMR. [c]DS for allyl groups per AGU analyzed by bromination of double bonds. [d]DS per AGU analyzed from XPS silica marker.[35,36] [e]DS per AGU analyzed from XPS nitrogen marker.[35,36] [f]Degree of surface charge and oxidation efficiency determined by conductometric titration of carboxylic acid groups, the theoretical maximum for wood cellulose crystal is 1.5 meq g^{-1}, which corresponds to every second glucose unit on the surface of cellulose crystal carrying a carboxylic acid group.[27] TEMPO oxidation is selective to primary alcohols (cellulose C6 position), and thus, there is only 1 reactive unit per 2 AGUs available on the crystal surface. [g]Result from Kjeldahl method. [h]Result estimated from XPS data. [i]Result from conductometric titration of carboxylic acid groups.

Estimation of the DS for TEMPO-oxidized NFC. The amount of carboxylic acid groups on TEMPO-oxidized pulp was determined by conductometric titration. For the sufficient fibrillation, the content of the carboxylic acid groups has to be higher than 0.7 meq g^{-1} of pulp, and the theoretical maximum of wood cellulose crystal is ~1.5 meq g^{-1}.[27] The content of the carboxylic acid groups of the TEMPO-oxidized pulp was over 0.9 meq g^{-1} of pulp (Table 1). The result corresponds to about 57% efficiency of oxidization of available C-6 hydroxyl groups on the surface of crystalline cellulose.[28]

Structural Analysis of Functionalized Fibrils by AFM. The morphology and fine structure of the spin-coated films of functionalized NFC were studied by AFM (Figure 1A, C, and F). The AFM images show that there are clear morphological differences between the different NFC types. Especially pronounced was the very fine structure of TEMPO–NFC, which is seen only in the small 1 × 1 μm image (Figure 1E, inset) compared to the more coarse amine–NFC and epoxy–NFC. The TEMPO–NFC fibers were more homogeneous in size and have fibrils of approximately 4 nm in diameter. Both amine–NFC and epoxy–NFC were more coarse and had larger variation in fibril heights (diameters) ranging from ~10 to 100 nm. However, the amine–NFC seemed to form a more densely packed and tighter film with more fiber–fiber interactions than epoxy–NFC. From AFM analysis we can conclude that all the NFC films were fully covering and porous.

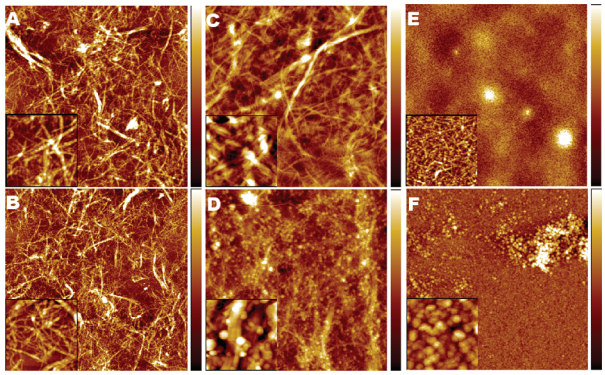

Figure 1. AFM topography images (10 × 10 μm) of surfaces made from negative controls without AP and from AP–NFC conjugates. Inserts are 1 × 1 μm magnifications of the images: (A) Epoxy–NFC control (maximum height 40 nm, insert maximum height 20 nm); (B) AP–epoxy–NFC conjugate (maximum height 40 nm, insert maximum height 25 nm); (C) Amine–NFC control (maximum height 200 nm, insert maximum height 50 nm); (D) AP–amine–NFC conjugate (maximum height 400 nm, insert maximum height 100 nm); (E) TEMPO–NFC control (maximum height 8 nm insert maximum height of 8 nm; (F) AP–TEMPO–NFC conjugate (maximum height of 100 nm, insert maximum height 50 nm).

Characterization of SFB–AP. Primary amines on the surface of AP were activated using SFB (see Scheme 1). The reaction between SFB and AP was confirmed by MALDI–TOF MS (Figure S1). Peak masses of AP (m/z = 47202.5) and SFB–AP (m/z = 48693.1) showed that on average 11.3 formylbenzoate (M = 132.109 Da) moieties were introduced per AP molecule. AP contains 29 Lys residues on its surface and, therefore, the efficiency of Lys modification was ~39%. Additionally a m/z = 97273.1 peak was detected, corresponding to a covalently cross-linked dimer of SFB–AP. Larger oligomers of SFB–AP were not seen and would likely be difficult to detect with MALDI–TOF. The concentration of SFB–AP was 1.13 g L^{-1}.

Characterization of AP Conjugated to NFC by the Different Routes. The three different (TEMPO, epoxy, and amine) AP–NFC conjugates were characterized by first spin coating the AP–NFC suspensions on silica surfaces. Negative controls prepared with NFC as described above were also made. Surfaces were assayed for enzymatic activity using the *p*-NPP substrate. The amount of immobilized AP was calculated from its activity compered to nonconjugated AP. The yield of conjugation reaction for AP was less than 1% because a large excess of AP was used in the reactions and reaction conditions were not optimized for this parameter.

The volume and amount of AP–NFC conjugate that was applied by spin coating was restricted by practical considerations. Too large volumes of NFC tended to give uneven surfaces, as did too high concentrations of NFC. In practice, the useful maximum concentration was for TEMPO 0.1 mg L^{-1} and for both epoxy– and amine–NFC 1.13 mg L^{-1}. The volume for all was 50 μL.

The spin coating procedure was repeated up to 11 times. Samples having different numbers of layers were then compared to each other. In Figure 2, the total amount of protein bound to the silicon surface after each successive coating layer is shown. The amount of protein added during each successive layer per mass of NFC is shown in Figure 3. For each of the different NFC derivatives there was an increase in

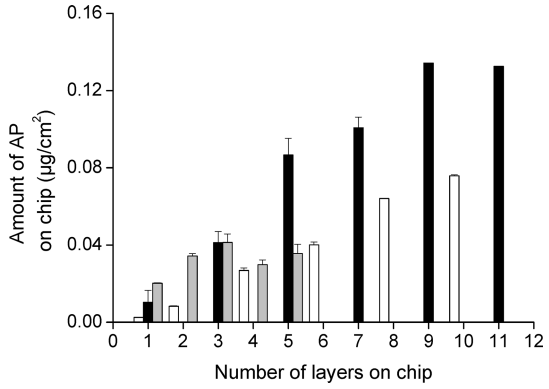

Figure 2. Enzymatic activity of spin-coated AP–NFC films showing the effect of spin coating multiple layers. The amount of AP increased for each successive spin-coated layer. The white bars represent epoxy–NFC, black bars represent TEMPO–NFC, and gray bars represent amine–NFC.

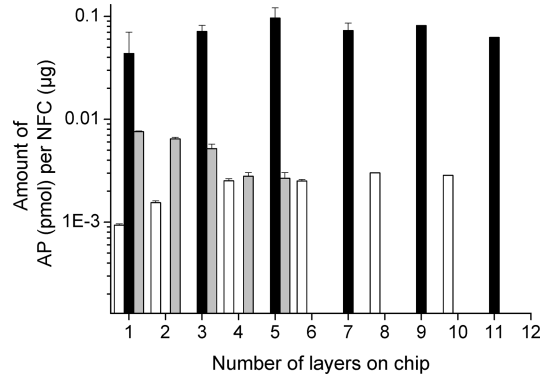

Figure 3. Immobilization density of AP (pmol) on each NFC derivative (μg). The values are calculated by determining the total activity of AP after each successive layer and dividing by the total NFC amount. White bars represent epoxy–NFC, black bars represent TEMPO–NFC, and gray bars represent amine–NFC.

activity for each successive layer. All three NFC derivatives showed good adhesion to underlying layers and to the PEI primed silicon surface. For each successive step, the limiting factor for the amount of NFC added was the practical limits set by the spin coating process. For the first three layers, the amine–NFC performed very well and allowed the largest amount of AP to be immobilized. Addition of more layers of amine–NFC after the first three ones did not increase activity. The TEMPO–NFC showed a linear increase in activity for each layer up to 11 layers. The epoxy–NFC showed less immobilized AP than the TEMPO, but unlike the amine–NFC, it showed a linear increase up to 10 subsequent layers. By comparing different samples, it could be concluded that the catalyst triethylamine, had no significant impact on the amount of conjugated AP for the epoxy–NFC.

TEMPO–NFC contained significantly higher amounts of reactive groups compared to the two other NFC derivatives (Table 1). The effect of higher degree of substitution is seen in over 10× higher capacity of bound protein (Figure 3, note logarithmic scale) per weight of cellulose. The higher surface to bulk ratio of TEMPO–NFC allowed a higher degree of AP conjugation, but the finely divided structure allowed application of only a much smaller amount of material in the spin coating. Therefore the total amount of protein that was possible to apply on the surface (Figure 2) was not as much higher as could have been expected based on the capacity (Figure 3).

Characterization by AFM (Figure 1) showed some additional differences between the different conjugates. Especially the TEMPO–NFC differed most markedly from the others by its distinct fine structure (Figure 1E). A difference between the different NFC derivatives is also that objects with a size corresponding to small clusters of protein molecules can be seen in the amine–NFC and TEMPO–NFC but not in the epoxy–NFC. This may be due to the difference in the chemistry used for the conjugation as discussed below.

The negative controls were analyzed for the possibility that noncovalently bound protein may be either physically entrapped in the NFC matrix or noncovalently coupled to the NFC by, for example, charge–charge interactions. In all the control surfaces, the AP activity was below the detection limits after washing the surfaces similarly as for the other samples. We noted, however, that if the surfaces were not properly washed (less than 1 h in buffered solution), a slight AP activity could be measured. It was also noted that the enzyme responsible for the activity was desorbing from the surfaces during activity measurements.

Long-Term Stability and Activity of AP–NFC Conjugates. The effect of the conjugation on the stability of AP with the different functionalized NFC was studied. Spin-coated films were stored in buffer at elevated temperatures and their activities monitored. Initial experiments showed that free AP in solution was stable at +4 °C for several months, but at 21 and 37 °C, the activity decreased rapidly. The activity decreased by 90% after 16 h at 21 °C and over 95% after 16 h in +37 °C. After 24 h at these temperatures, almost no activity could be detected. In contrast, all conjugated AP–NFC combinations showed a marked increase in stability. After 168 h at 21 °C, all three conjugates showed no decrease in AP activity compared to the initial AP activity on the films measured immediately after spin coating and washings. After 168 h at 37 °C, the AP TEMPO–NFC, AP amine–NFC, and AP epoxy–NFC conjugates showed 27, 18, and 26% of their original activity, respectively.

Conjugation of hydrocortisone to AP, and anti–hydrocortisone antibody purification. MALDI–TOF MS data showed that hydrocortisone–AP conjugates had the conjugation degree of 6–10 hydrocortisones per 1 AP monomer. After purifications, the concentration of the final hydrocortisone–AP conjugate was 1.36 g L^{-1} in PBS. The anti–hydrocortisone antibody concentration after metal affinity chromatography purification was 3 g L^{-1} in PBS.

Antibody Conjugation to TEMPO–NFC and Its Immunological Detection. Based on the efficiency of conjugating and immobilizing AP, TEMPO–NFC was chosen for further studies for immobilizing antibodies to surfaces. Anti-hydrocortisone antibody was conjugated to TEMPO–NFC and spin-coated with one and two layers on a silicon surface. Hydrocortisone conjugated to AP was used as the antigen for analyzing the functionality of the anti-hydrocortisone antibody conjugated to TEMPO–NFC. The use of this AP conjugate gave the advantage that bound hydrocortisone could be detected directly by the AP + *p*-NPP reaction. In a negative control, the anti-hydrocortisone antibody was left out. The results of the functional analysis are shown in Figure 4. The bound hydrocortisone–AP conjugate was estimated to be 11 ng on both one and two layered surfaces based on the enzymatic activity of AP (Figure 4). The negative control

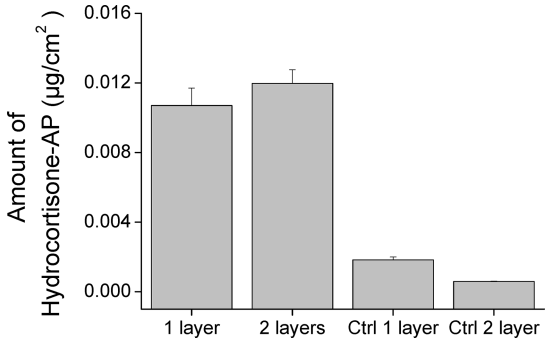

Figure 4. Immobilization of anti-hydrocortisone antibody onto a surface by TEMPO-oxidized NFC and its detection with hydrocortisone–AP conjugate. The amount of hydrocortisone–AP conjugate per surface area on both one- and two-layered silicon surfaces is very similar.

without anti-hydrocortisone antibody showed between 24 (two layers) and 6 (one layer) times lower activity compared to the samples containing all components. The higher background for the sample with one coating may be due to some residue exposure of the underlying PEI surface.

Nonspecific Binding of Proteins to NFC and PEI Surfaces, a QCM-D Study. The nonspecific adsorption of proteins, in our case, BSA, AP, SFB–AP, and hydrocortisone–AP, to unmodified NFC and PEI surfaces was studied using QCM-D. Results presented in Table 2 showed very low adsorption of all the proteins on NFC and also on PEI. The negative change in frequency, which indicates the positive mass change detected on the sensor surface, was less than 2.2 Hz for all protein samples during the contact time of 2–3 h time, indicating no significant adsorption. This very low adsorption of proteins to cellulose surface show that NFC itself has a low background effect in assays where proteins are immobilized for example on solid surfaces.

Table 2. Amounts of BSA, AP, Hydrocortisone–AP, and SFB–AP Bound nonspecifically to PEI and NFC Surfaces in PBS pH 7.2[a]

protein	$\Delta f/\Delta D$ on PEI	$\Delta f/\Delta D$ on NFC	ng/cm^2 PEI/NFC[b]
BSA	−1.3/0.15	−0.6/0.04	23.0/10.6
AP	−2.16/0.05	−1.1/-0.04	32.2/19.5
hydrocortisone–AP	−0.33/-0.01	0/0.01	5.84/0
SFB–AP	−0.9/0.06	−0.45/0.04	15.9/7.97

[a] f_0 = 5 Hz, n = 3, f_3/n, time 2–3 h, C = 0.177 mg m^{-2} Hz^{-1}. [b] Values calculated by Sauerbrey equation $\Delta m = -(C\Delta f/n)$.[44]

DISCUSSION

We show here that nanocellulose provides an efficient strategy for immobilizing proteins on surfaces. The properties of NFC allow an approach that is different from typical immobilization protocols[5,7,8] because the covalent linkage of the protein can be performed in solution using suspended NFC and the immobilization itself relies on the physical interactions of NFC that lead to film formation on surfaces. The physical interactions of NFC are based on the noncovalent networks that the long cellulose fibrils form when spread on surfaces and their interactions through hydrogen bonding.

The protein–NFC films had a nanoporous structure that had an influence on how molecules of different sizes can interact with the immobilized proteins. The chemistry of how NFC was functionalized had a significant impact on how the protein was immobilized and how the bioactive films were formed, but the immobilized protein itself did not significantly alter the film-forming capability of NFC. The way NFC formed films and coatings depended significantly on its size distribution, that is, processing history. Also, the three alternative ways of introducing functional groups on the NFC surface all lead to a different characteristic of the resulting NFC–protein conjugates. The amount of reactive groups, fibril dimensions (specific surface area), and conjugation chemistry used for linking enzymes to NFC derivatives all have an impact on the degree of conjugation.

The degree of functionalization for the different NFC derivatives was determined according to the most suitable method for each functional group. Although the methods differed from one another, we can compare the amount of functional groups on the different NFC derivatives as follows. In the case of epoxy–NFC, the degree of functionalization of 0.06 corresponds to 6% of modified anhydroglucose units (AGUs). In the case of amine–NFC, the DS of 0.2 corresponds to 20% of modified AGUs. In the case of TEMPO–NFC, the reaction is regioselective to primary alcohols (in cellulose C6 hydroxyls) and the reaction acts only on the fibril surface. Thus, the degree of functionalization only considers surface C6 hydroxyls. The degree of surface functionalization of ∼0.9 meq g^{-1} pulp corresponds to roughly 57% of modified primary alcohols on cellulose crystal.[27] In our case, therefore, the TEMPO–NFC was the most highly substituted and epoxy–NFC was the least.

The procedures of conjugating protein to both TEMPO–NFC and amine-functionalized NFC involve several reaction steps, while the conjugation to epoxy-functionalized NFC proceeded in a single step (Scheme 1). The reaction times for conjugation to amine- and TEMPO-functionalized NFC was much faster than the conjugation to epoxy-functionalized NFC. The epoxy route also gave the lowest density of immobilized AP. From literature, it is previously known that the reactions to epoxy-activated supports are very slow, leading for example to attempts to increase reaction rates by salt-induced aggregation.[6] The efficiency of epoxy immobilization in this work was comparable to previously published results .[46]

Comparing the AFM images of the protein–NFC films (Figure 1), we note that the surfaces with proteins conjugated to amine- and TEMPO-functionalized NFC show globular aggregates of molecules with the diameter of about 70 nm. Such aggregates are not seen in the epoxy-functionalized NFC. Because the sizes of the aggregates are larger than is expected for the natural dimeric form of AP (5–6 nm), it is likely that these aggregates are small clusters of AP enzyme. In both strategies for immobilizing to amine and TEMPO-functionalized NFC, the side reactions can lead to the formation of chemically cross-linked AP enzyme. When immobilizing to amino groups, the intermediate step of making SFB–AP leads to the modification of about 40% of the lysine residues in AP. As the formed formylbenzoate group is reactive toward amino groups, the cross-linking of individual SFB–AP molecules to larger oligomers is possible and at least the dimer form of AP was confirmed by MALDI–TOF (see Figure S1). This cross-linking is likely to lead a mechanism where the immobilized units are oligomeric clusters instead of monomers of AP to

SANH−NFC. Similarly, in the case of TEMPO−NFC, a carboxyl acid activating reagent EDC/s-NHS mixture was used. Excess activator was not removed prior to addition of AP because of the poor stability of the activated carboxylic acid group in aqueous solution. As AP was added to the activation mixture it is possible that some excess of activator reacted with surface exposed aspartic and glutamic acid residues on AP (see Figure S6) and, thus, resulting in cross-linking of AP protein molecules to larger clusters. Such clusters of AP or individual AP molecules could not be identified in epoxy−NFC films. The clustering is not expected in the epoxy−NFC case due to the nature of the chemistry used for conjugation. Individual AP molecules would probably be hard to identify in the fibril network due to their small size and much lower modification density compared to amine- and TEMPO-functionalized NFC.

The formation of such small clusters would explain the globular aggregates seen in the AFM images and could also partly explain the increased efficiency of immobilization to amine and TEMPO functionalized NFC, since for every functional group a cluster of AP could bind instead of individual molecules as in the epoxy functionalized case. The cross−linking of enzymes together can also aid the stabilization and preservation of enzyme activity. Both conjugation methods on TEMPO− and amine−NFC combine two features that are thought to be very effective in protein immobilization and enzyme stability preservation; the multipoint covalent immobilization of protein[5] and carrier-bound cross-linked enzymatic aggregation.[2] In our case, the multipoint covalent attachment occurs both between individual enzyme molecules and between the enzyme and the solid support (in our case, NFC), resulting in a system where the protein is simultaneously covalently bound to the carrier as well as cross-linked to small clusters. However, increased stability of AP was also seen for the epoxy−NFC, which shows that the NFC structure is a generally biocompatible environment for proteins. It is likely that the hydrophilic nature of cellulose and its rigid structure are reasons for this. It was also shown that the NFC films have very low nonspecific binding which is a clear advantage over many polymer matrixes and other functional surfaces used for immobilization.[47] The low protein binding to NFC may also be a contributing factor for the biocompatibility of the NFC. Another clear effect of the protein conjugation to NFC was the observed increase in stability. Increase in stability has been described to occur for several enzymes and has been attributed to intramolecular cross-linking.[2] In this work, we did not investigate mechanism of the increase of stability in a systematic way. However, we observe that in accordance with published work, multipoint cross-linking[5] can result in increased stability and that this conclusion is in accordance with the other results of this work. Previously has also been shown that the cross-linking chemistry and the microenvironment of the carrier has an effect on the inactivation and stabilization of enzymes.[3] It has been shown that for better stability covalent immobilization is a more advantageous immobilization method over adsorption and that hydrophilic carriers are more advantageous that hydrophobic ones. These results are in line with our findings of increased stability with protein conjugation to NFC.

When applying layers of AP−NFC by spin coating an increase in enzymatic activity was seen for each successive layer. As a general trend, the measured activity of AP with *p*-NPP as the substrate increased with successive layers, suggesting that the layers had a porous structure that allowed the transport of the small substrate through the network and that underlying layers contributed to the total activity (Figures 2 and 3). However, clear differences between the different types of NFC were observed. Initially the NFC with AP coupled to amine−NFC showed a greater amount of AP activity, but after about four layers the efficiency declined (Figure 3). The reason for this is likely to be that a densely packed film was formed which did not allow the penetration of even the small *p*-NPP molecule deeper into the structure of the film. Therefore the response was seen only from the topmost layers. The tighter packing of amine functionalized NFC fibrils in the film can be seen in the AFM images (Figure 1). On the other hand, the epoxy−NFC and TEMPO−NFC showed a linear and continuous increase in the amount of immobilized protein, suggesting a more porous or loosely packed film. TEMPO−NFC has a large aspect ratio, is very even in size distribution, and contains a large number of carboxyl groups on its surface. The finer structure of the TEMPO−NFC is also clear from the AFM images (Figure 1), thus, making the film forming and swelling properties very good. The apparently less dense film structure of epoxy−NFC compared to amine−NFC may be that the chemical modification of epoxy−NFC lead to a greater reduction of hemicelluloses (alkaline treatment) as well as to an introduction of hydrophobic groups on the fibrils and, therefore, to a poorer or more coarse film structure compared to amine−NFC.[48]

The experiments using immobilized antibodies did not show a significant increase in binding of antigens with additional deposited layers of antibody−NFC conjugate. The density of immobilization detected for the first layer (11 ng on antibody conjugated TEMPO−NFC) corresponded to the density achieved using the direct immobilization of AP. Because additional layers did not increase the response, we conclude that large proteins (such as AP) do not diffuse through the TEMPO−NFC film structure. An AP monomer is a globular protein with a diameter of approximately 5−6 nm in its active dimer form. This shows that, although the NFC conjugation and immobilization is versatile in functioning for different types of targets, the porosity[21] of the NFC layer and the structure of the analytes have a dependency that affects the overall performance of the system and should be taken into account in the design. Thus, the TEPMO−NFC immobilization can be advantageous in systems where a large density is achieved due to the porosity of the surface layer and its availability for small molecules. The exclusion of macromolecules can be beneficial when targeting small molecules, but may be a limitation in applications where macromolecules are targeted.

■ CONCLUSIONS

In this work we have shown that NFC derivatives can be used as matrixes for conjugation and stabilization of enzymes and proteins and that bioactive films immobilizing the proteins on surfaces are readily formed by these protein−NFC conjugates. Typically it is technically challenging to perform chemical reactions on surfaces or on surface-immobilized polymers because of slow kinetics and difficulties to mix reagents efficiently, leading to slow reactions and low yields. Scale-up and process design is also problematic for large solid surfaces. We therefore propose that the procedure described here, to first perform chemical reactions in solution and then spread the mixture on the target surface, will provide a technically more feasible procedure. The conjugation reactions can be performed under well-controlled mild aqueous conditions, mixing, and temperature, while spreading of the mixture for immobilization

could be readily automated by various printing or coating technologies. The work is also a demonstration that cellulose in its highly fibrillated NFC form shows highly desirable properties that lead to new methods in technology.

■ ASSOCIATED CONTENT

Supporting Information

(Figure S1) MALDI−TOF MS sample preparation for SFB−AP with MALDI−TOF MS spectra of AP and SFB−AP (Figure S1 and S2); description of allylation of MFC prior to epoxidation and the ^{13}C CP/MAS NMR spectra of allylated MFC (Figure S2 and S3); descriptions of the determination of functionalization degree of amine−NFC accompanied by XPS spectra (Figure S3); and elemental concentrations (Table S3) of NFC and amine−NFC. This material is available free of charge via the Internet at http://pubs.acs.org.

■ AUTHOR INFORMATION

Corresponding Author

*Tel.: +358 40 180 3812. Fax: +385 02 722 7071. E-mail: ext-suvi.arola@vtt.fi.

Notes

The authors declare no competing financial interest.

■ ACKNOWLEDGMENTS

We thank the Finnish Centre for Nanocellulosic Technologies for providing the nanocellulose, Kari Kammiovirta, Vuokko Liukkonen, and Evanthia Monogioudi for technical assistance. Dr. Leena−Sisko Johansson is gratefully acknowledged for XPS analysis. The Academy of Finland, the Finnish Funding Agency for Technology and Innovation (TEKES), UPM−Kymmene Corporation, and Graduate School for Biomass Refining are thanked for funding.

■ REFERENCES

(1) Stephanopoulos, N.; Francis, M. B. *Nat. Chem. Biol.* **2011**, *7*, 876−884.
(2) Cao, L. *Curr. Opin. Chem. Biol.* **2005**, *9*, 217−226.
(3) Hwang, S.; Lee, K.-T.; Park, J.-W.; Min, B.-R.; Haam, S.; Ahn, I.-S.; Jung, J.-K. *Biochem. Eng. J.* **2004**, *17*, 85−90.
(4) Rusmini, F.; Zhong, Z.; Feijen, J. *Biomacromolecules* **2007**, *8*, 1775−1789.
(5) Mateo, C.; Grazu, V.; Palomo, J. M.; Lopez-Gallego, F.; Fernandez-Lafuente, R.; Guisan, J. M. *Nat. Protoc.* **2007**, *2*, 1022−1033.
(6) Wheatley, J. B.; Schmidt, D. E. Jr *J. Chromatogr., A* **1993**, *644*, 11−16.
(7) Ong, E.; Gilkes, N. R.; Warren, R. A. J.; Miller, R. C.; Kilburn, D. G. *Nat. Biotechnol.* **1989**, *7*, 604−607.
(8) Kumar, S.; Nahar, P. *Talanta* **2007**, *71*, 1438−1440.
(9) Klemm, D.; Heublein, B.; Fink, H.-P.; Bohn, A. *Angew. Chem., Int. Ed.* **2005**, *44*, 3358−3393.
(10) Fengel, D.; Wegener, G. *Wood: Chemistry, Ultrastructure, Reactions*; Walter de Gruyter: Berlin, NY, 1984; pp 6−25.
(11) Klemm, D.; Kramer, F.; Moritz, S.; Lindström, T.; Ankerfors, M.; Gray, D.; Dorris, A. *Angew. Chem., Int. Ed.* **2011**, *50*, 5438−5466.
(12) Nakagaito, A. N.; Yano, H. *Appl. Phys. A: Mater. Sci. Process.* **2005**, *80*, 155−159.
(13) Pääkkö, M.; Ankerfors, M.; Kosonen, H.; Nykänen, A.; Ahola, S.; Österberg, M.; Ruokolainen, J.; Laine, J.; Larsson, P. T.; Ikkala, O.; Lindström, T. *Biomacromolecules* **2007**, *8*, 1934−1941.
(14) Paakko, M.; Vapaavuori, J.; Silvennoinen, R.; Kosonen, H.; Ankerfors, M.; Lindstrom, T.; Berglund, L. A.; Ikkala, O. *Soft Matter* **2008**, *4*, 2492−2499.
(15) Zugenmaier, P. *Prog. Polym. Sci.* **2001**, *26*, 1341−1417.
(16) Herrick, F. W.; Casebier, R. L.; Hamilton, J. K.; Sandberg, K. R. *J. Appl. Polym. Sci.: Appl. Polym. Symp.* **1983**, *37*, 797−813.
(17) Turbak, A. F.; Snyder, F. W.; Sandberg, K. R. *J. Appl. Polym. Sci.: Appl. Polym. Symp.* **1983**, *37*, 815−827.
(18) Olsson, R. T.; Azizi Samir, M. A. S.; Salazar Alvarez, G.; Belova, L.; Strom, V.; Berglund, L. A.; Ikkala, O.; Nogues, J.; Gedde, U. W. *Nat. Nanotechnol.* **2010**, *5*, 584−588.
(19) Varjonen, S.; Laaksonen, P.; Paananen, A.; Valo, H.; Hahl, H.; Laaksonen, T.; Linder, M. B. *Soft Matter* **2011**, *7*, 2402−2411.
(20) Eichhorn, S.; Dufresne, A.; Aranguren, M.; Marcovich, N.; Capadona, J.; Rowan, S.; Weder, C.; Thielemans, W.; Roman, M.; Renneckar, S.; Gindl, W.; Veigel, S.; Keckes, J.; Yano, H.; Abe, K.; Nogi, M.; Nakagaito, A.; Mangalam, A.; Simonsen, J.; Benight, A.; Bismarck, A.; Berglund, L.; Peijs, T. *J. Mater. Sci.* **2010**, *45*, 1−33.
(21) Ahola, S.; Salmi, J.; Johansson, L. S.; Laine, J.; Österberg, M. *Biomacromolecules* **2008**, *9*, 1273−1282.
(22) Wagberg, L.; Decher, G.; Norgren, M.; Lindstrom, T.; Ankerfors, M.; Axnas, K. *Langmuir* **2008**, *24*, 784−795.
(23) Henriksson, M.; Berglund, L. A.; Isaksson, P.; Lindström, T.; Nishino, T. *Biomacromolecules* **2008**, *9*, 1579−1585.
(24) Ahola, S.; Turon, X.; O'sterberg, M.; Laine, J.; Rojas, O. J. *Langmuir* **2008**, *24*, 11592−11599.
(25) Nakagaito, A.; Yano, H. *Cellulose* **2008**, *15*, 323−331.
(26) Syverud, K.; Stenius, P. *Cellulose* **2009**, *16*, 75−85.
(27) Saito, T.; Kimura, S.; Nishiyama, Y.; Isogai, A. *Biomacromolecules* **2007**, *8*, 2485−2491.
(28) Saito, T.; Nishiyama, Y.; Putaux, J.-L.; Vignon, M.; Isogai, A. *Biomacromolecules* **2006**, *7*, 1687−1691.
(29) Maunu, S. L. *Prog. Nucl. Magn. Reson. Spectrosc.* **2002**, *40*, 151−174.
(30) Heinze, T.; Lincke, T.; Fenn, D.; Koschella, A. *Polym. Bull.* **2008**, *61*, 1−9.
(31) Huijbrechts, A. M. L.; Haar, R. t.; Schols, H. A.; Franssen, M. C. R.; Boeriu, C. G.; Sudhölter, E. J. R. *Carbohydr. Polym.* **2010**, *79*, 858−866.
(32) Holmberg, M.; Berg, J.; Stemme, S.; Ödberg, L.; Rasmusson, J.; Claesson, P. *J. Colloid Interface Sci.* **1997**, *186*, 369−381.
(33) Schaub, M.; Wenz, G.; Wegner, G.; Stein, A.; Klemm, D. *Adv. Mater.* **1993**, *5*, 919−922.
(34) Tammelin, T.; Saarinen, T.; Österberg, M.; Laine, J. *Cellulose* **2006**, *13*, 519−535.
(35) Johansson, L.-S.; Tammelin, T.; Campbell, J. M.; Setala, H.; Osterberg, M. *Soft Matter* **2011**, *7*, 10917−10924.
(36) Andresen, M.; Johansson, L.-S.; Tanem, B. S.; Stenius, P. *Cellulose* **2006**, *13*, 665−677.
(37) Hermanson, G. T. *Bioconjugate Techniques*, 2nd ed.; Academic Press: New York, 2008; pp 582−626.
(38) Azzam, F.; Heux, L.; Putaux, J.-L.; Jean, B. *Biomacromolecules* **2010**, *11*, 3652−3659.
(39) Hermanson, G. T. *Bioconjugate Techniques*, 2nd ed.; Academic Press: New York, 2008; p 666−706.
(40) Pulli, T.; Höyhtyä, M.; Söderlund, H.; Takkinen, K. *Anal. Chem.* **2005**, *77*, 2637−2642.
(41) Turunen, L.; Takkinen, K.; Söderlund, H.; Pulli, T. *J. Biomol. Screen.* **2009**, *14*, 282−293.
(42) Takkinen, K.; Laukkanen, M.-L.; Sizmann, D.; Alfthan, K.; Immonen, T.; Vanne, L.; Kaartinen, M.; Knowles, J. K. C.; Teeri, T. T. *Protein Eng., Des. Sel.* **1991**, *4*, 837−841.
(43) Nevanen, T. K.; Söderholm, L.; Kukkonen, K.; Suortti, T.; Teerinen, T.; Linder, M.; Söderlund, H.; Teeri, T. T. *J. Chromatogr., A* **2001**, *925*, 89−97.
(44) Höök, F.; Rodahl, M.; Brzezinski, P.; Kasemo, B. *Langmuir* **1998**, *14*, 729−734.
(45) Rodahl, M.; Hook, F.; Krozer, A.; Brzezinski, P.; Kasemo, B. *Rev. Sci. Instrum.* **1995**, *66*, 3924−3930.
(46) Chen, B.; Pernodet, N.; Rafailovich, M. H.; Bakhtina, A.; Gross, R. A. *Langmuir* **2008**, *24*, 13457−13464.
(47) Ahluwalia, A.; De Rossi, D.; Ristori, C.; Schirone, A.; Serra, G. *Biosens. Bioelectron.* **1992**, *7*, 207−214.

(48) Iwamoto, S.; Abe, K.; Yano, H. *Biomacromolecules* **2008**, *9*, 1022−1026.

Supporting Information for

Immobilization–stabilization of proteins on nanofibrillated cellulose derivatives

Suvi Arola[ac], Tekla Tammelin[b], Harri Setälä[b], Antti Tullila[a] and Markus B. Linder[a]*

[a]VTT, Technical Research Centre of Finland, Bio and process technology, Tietotie 2, FIN–02044 VTT, Finland, [b]VTT, Technical Research Centre of Finland, Energy and Pulp&Paper, Biologinkuja 7, FIN–02044 VTT, Finland, [c]Aalto University School of Science and Technology, Department of Applied Physics, P.O. Box 15100, FI–00076 Aalto, Finland

Ext-suvi.arola@vtt.fi

RECEIVED DATE (to be automatically inserted after your manuscript is accepted if required according to the journal that you are submitting your paper to)

Suvi Arola (née Varjonen), VTT Technical Research Centre of Finland, Tietotie 2, FIN–02044 VTT, Finland, Mobile: +358 40 180 3812, Fax: +385 02 722 7071, Email: Ext-suvi.arola@vtt.fi

Supporting Information

Supporting information contains S1) MALDI–TOF MS sample preparation for SFB–AP with MALDI–TOF MS spectra of AP and SFB–AP (Figure S1), S2) description of allylation of MFC prior to epoxidation and the ^{13}C CP/MAS NMR spectra of allylated MFC (Figure S2), and S3) descriptions of the determination of functionalization degree of amine–NFC accompanied by XPS spectra (figure S3) and elemental concentrations (Table S3) of NFC and amine–NFC.

S1 MALDI–TOF analysis of AP and SFB–AP. In order to prepare the MALDI–TOF samples of AP and SFB–AP TA–solution was prepared by diluting 0.1 % trifluoroacetic acid in MilliQ–water in 1:1 proportion to acetonitrile. A saturated solution of sinapic acid (Fluka, 49508–10MG–F) in TA–solution was used as matrix. Protein samples were diluted in TA–solution. 1 µl of 1:1 ration of protein/matrix mixture was spotted on a ground steel target plate and flight times were measured. The standard used in the measurements was Protein Calibration Standard II (Brukser Daltonics, 207234). The MALDI–TOF spectra of SFB–AP and AP are shown in figure S6. From the spectra we can see that the difference in mass between AP and SFB–AP is m/z 1496.4. The reaction of SFB and lysine residues attaches formylbenzoate to the lysine residue via peptide bondage. One attached formylbenzoate yields a rise of mass by 132.1 Da. This means that in average there are 11.3 modified lysine groups on each AP molecule. In the SFB–AP spectra there is another peak at m/z 97273.143. This can correspond to a dimmer of AP with 21.8 modified lysines. As aldehydes can react with primary amines to produce imines the formation of covalently bound dimers and even larger oligomers is possible in the case of SFB–AP.

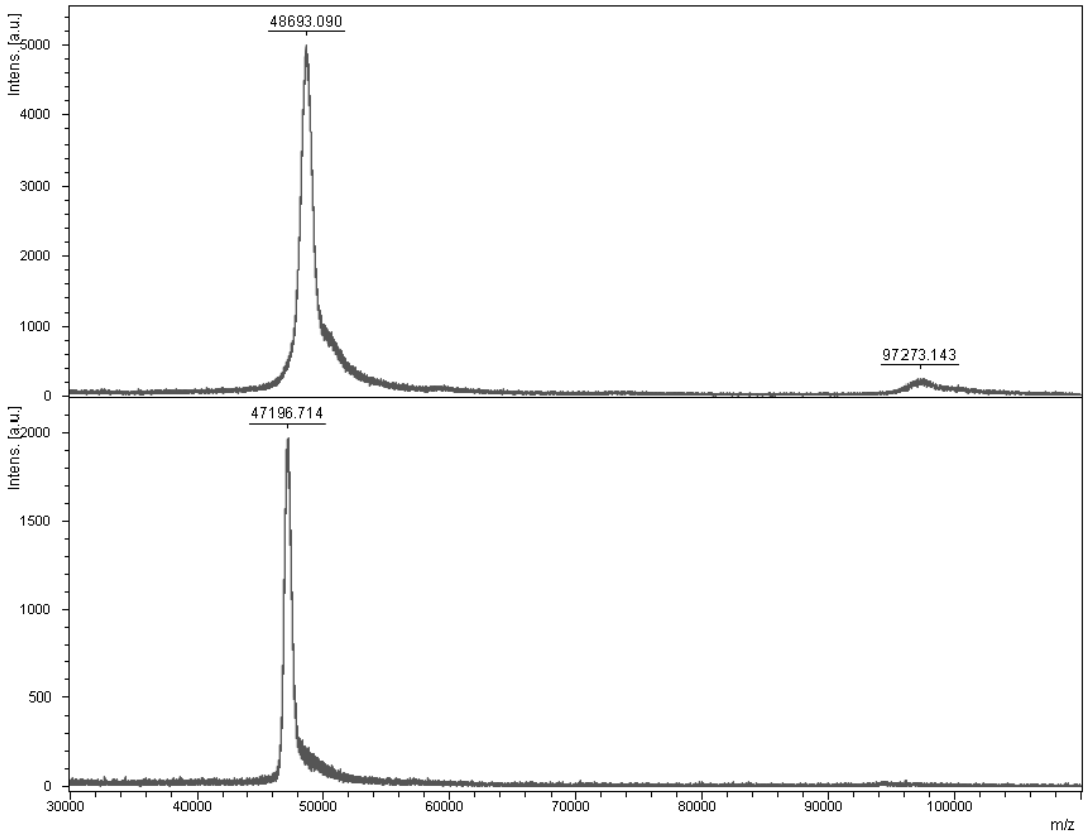

Figure S1. MALDI–TOF spectra of SFB–AP (top) and AP (bottom). SFB–AP monomer carrying ~11.3 formylbenzoate molecules is seen at m/z 48693.090 and a dimer of it at m/z 97273.143. AP molecule is seen at m/z 47196.714.

S2 ^{13}C CP/MAS NMR spectra of epoxy functionalized microfibrillated cellulose (epoxy–MFC). The allylation of MFC was done in two steps because in the first reaction the soluble hemicelluloses disturb the reaction. In the first step 40% of hemicelluloses are removed and a very low yield of butyl and allyl modification is achieved ($DS_{butyl+allyl}$ = 0.01) which can be seen from the left hand side NMR spectra. The amount of allyl groups is very low and it falls below the detection limits of the method thus butyl peaks are used for the determination of modification extent. After the second allylation step the extent of allyl modification can be determined from the allyl peaks at 140–120 ppm. The DS_{allyl} after two step allylation was calculated to be 0.066 by combining the integrated areas of both allyl peaks and comparing it to the anomeric C1 peak in cellulose.

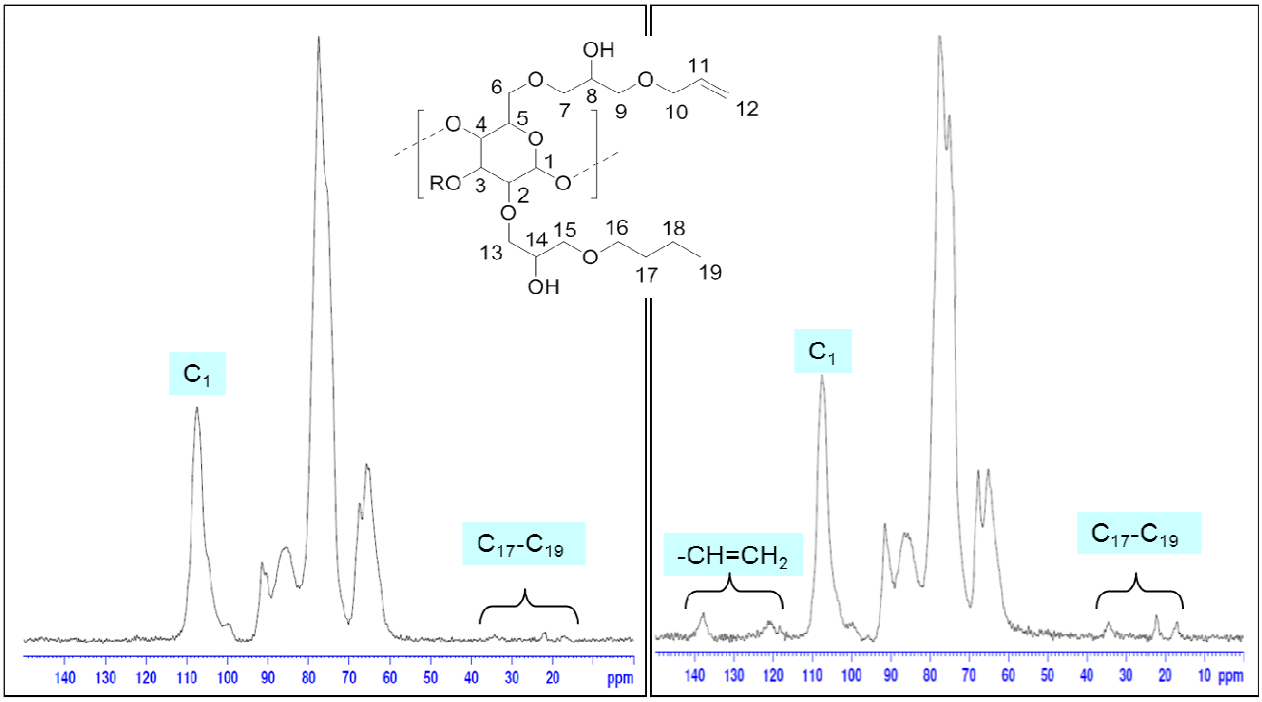

Figure S2. The ^{13}C CP/MAS NMR spectra of MFC fibers after the first allylation step (left) and after the second allylation step (right). A schematic drawing of the functional groups attached on a glucose unit of cellulose chain is presented to ease the interpretation of the spectra.

S3 Determining the degree of functionalization of amine functionalized nanofibrillated cellulose (amine–NFC). The degree of amine functionalization was calculated from the surface silicon and surface nitrogen content analyzed by X–Ray photoelectron spectroscopy (XPS) as described in Johansson et al.[1] Figure S2 shows XPS survey spectra peaks due to emission of O 1s, C 1s, N 1s, Si 2s and Si 2p electrons. Survey scans were used in determination of surface elemental concentrations. O 1s (oxygen) and C 1s (carbon) originate from cellulose whereas N 1s (nitrogen), Si 2s and Si 2p (silica) are markers for successfully aminated nanocellulose samples. Table S2 shows the elemental concentrations and relative abundance of different carbon bonds achieved by curve fitting of carbon C1 s spectra.[2,3] The degree of amination was calculated from the nitrogen and silicon content. The surface content of nitrogen was 1.7 % and the surface content of silicon was 1.5 % for amine–NFC, corresponding to surface substitution values of 0.21 for nitrogen marker and 0.19 for silica marker, respectively.

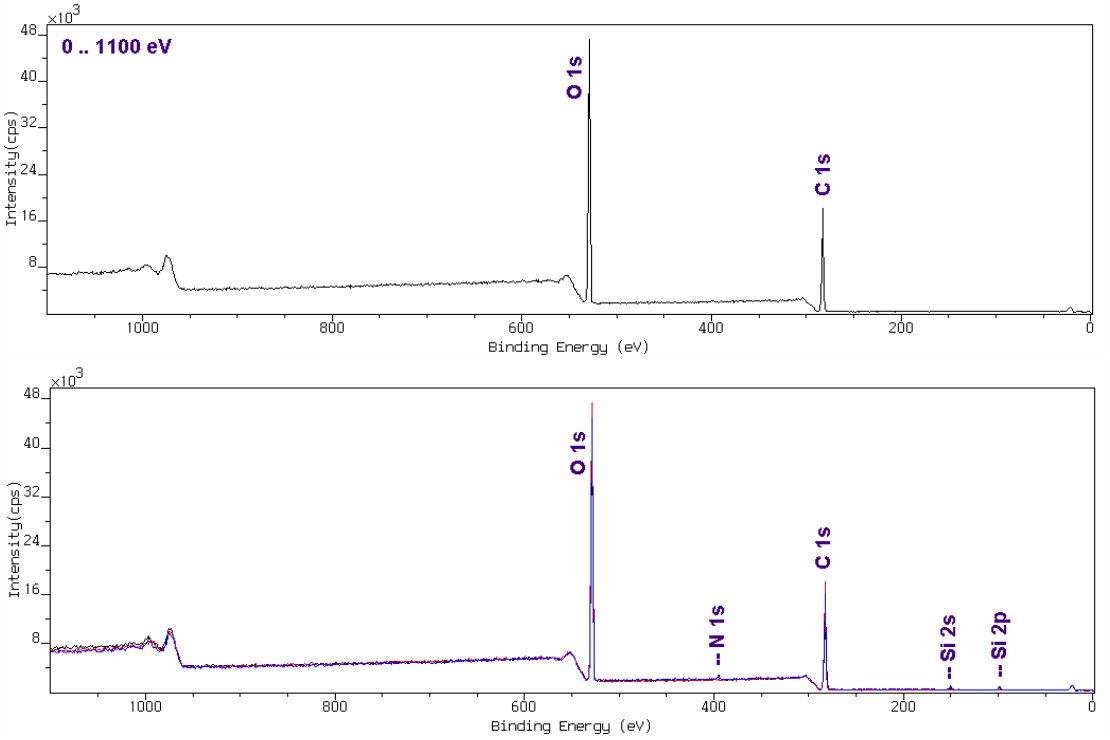

Figure S3. Low resolution XPS survey spectra recorded for unmodified fluidized NFC (top panel) and for amine–NFC (bottom panel).

Table S3. XPS data for NFC and amine–NFC.

	Elemental concentration (at-%)				Relative abundance of carbon bonds (at-%)			
Sample	O 1s	C1s	N1 s	Si 2p	C-C	C-O	O-C-O	C=O
Unmodified NFC	43.4	56.4	0.1	0	3.8	76.8	18.6	0.8
Aminated-NFC	41.5	55.3	1.7	1.5	8.9	72.9	17.4	0.8

References

(1) Johansson, L.-S.; Tammelin, T.; Campbell, J. M.; Setala, H.; Osterberg, M. *Soft Matter* **2011**, *7*, 10917-10924.

(2) Beamson, G.; Briggs, D. *High resolution XPS of organic polymers : the Scienta ESCA300 database*; Wiley: Chichester [England]; New York, 1992.

(3) Koljonen, K.; Österberg, M.; Johansson, L. S.; Stenius, P. *Colloids Surf., A* **2003**, *228*, 143-158.